Supplementary material 1

Nitrogen cycling dynamics under altering redox conditions during sapropels S1 and the ambiguous S2 in the Eastern Mediterranean Sea

Zoë R. van Kemenade[a], Anna Cutmore[a], Rick Hennekam[a], Ellen. C. Hopmans[a], Marcel T.J. van der Meer[a], Meryem Mojtahid[b], Frans J. Jorissen[b], Nicole J. Bale[a], Gert-Jan Reichart[a, c], Jaap S. Sinninghe Damsté[a, c], Darci Rush[a]

[a] NIOZ Royal Netherlands Institute for Sea Research, Landsdiep 4, 1797 SZ, 't Horntje, The Netherlands

[b]University of Angers, UMR 6112, 2 Bd Lavoisier, 49045 Angers Cedex, France

[c] Department of Earth Sciences, Utrecht University, Princetonlaan 8a, 3584 CB Utrecht, the Netherlands

S1.1 Core chronology

The 64PE406-E1 chronology is based on the well-dated sapropel boundaries (see Hennekam et al., 2020; Clarkson et al., 2021). For our study, the age model is updated through cross-comparison of the $\delta^{18}O$ of *Globigerinoides ruber* to well-dated cores (MS21 and LC21; Grant et al., 2012; Zwiep et al., 2018, respectively) and by correlation to the Soreq cave $\delta^{18}O$. The stable isotopes of crushed *G. ruber* shells were analysed using a Kiel-IV device coupled to a Thermo-Finnigan MAT253. A standard run consisted of 38 samples interspersed with 5 in-house standards (NFHS-1) and 4 international carbonate standards (NBS-19). The isotope ratios are given relative to the Vienna Pee Dee Belemnite (VPDB) standard using the delta notation. Results were normalized against NBS19 ($\delta^{18}O$ = -2.20‰, $\delta^{13}C$ = 1.95‰) and in-house standard NFHS-1 ($\delta^{18}O$ = 1.148‰, $\delta^{13}C$ = 0.854‰). The mean external reproducibility was better than ±0.05‰.

The here presented $\delta^{18}O$ record of *G. ruber* allows to further fine tune our existing age model for our target interval from 0-60 kyr BP. Following the reasoning of Grant et al. (2012), *G. ruber* $\delta^{18}O$ correlates well to Soreq speleothem $\delta^{18}O$ as both are affected by $\delta^{18}O$ changes of Mediterranean surface waters. Hence, two tie-points were added between 64PE406-E1 *G. ruber* $\delta^{18}O$ to the Soreq $\delta^{18}O$ at ~68 and ~55 kyr BP (Fig. S1). Moreover, *G. ruber* $\delta^{18}O$ records from the Eastern Mediterranean Sea region show similar variability with almost identical absolute values outside sapropel intervals (see, e.g., Rohling et al., 2017). This is also the case for core 64PE406-E1, and therefore we added five tie-points in the interval from 10-44 kyr between our piston core and well-dated (through ^{14}C and tephra) cores MS21 and LC21 (Fig. S1).

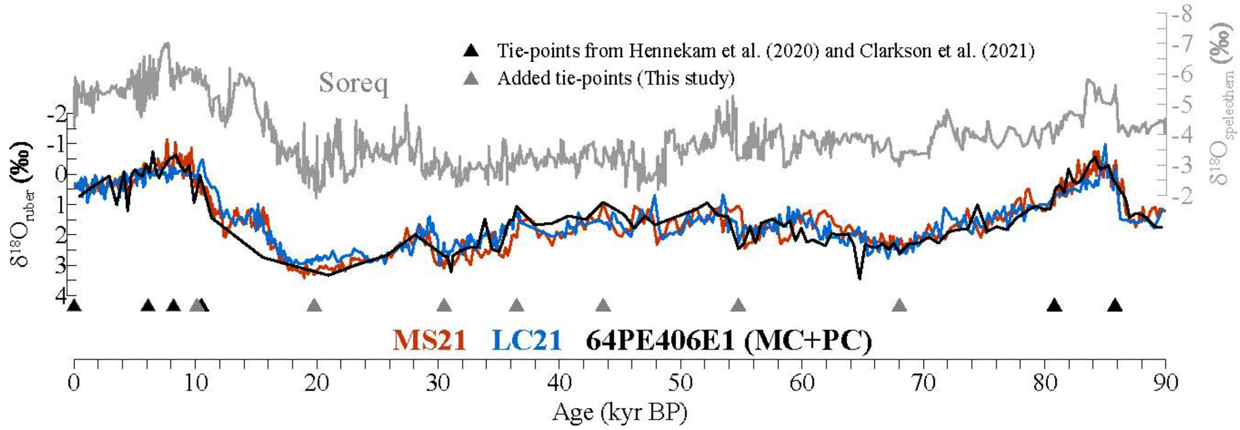

Figure S1. $\delta^{18}O$ values [‰ VPDB] of *G. ruber* in core MS21 (red), LC21 (blue) and multi, - and piston core of site 64PE406-E1 (black). Soreq speleothem $\delta^{18}O$ [‰ VPDB] is shown in grey. Tie points between 64PE406-E1 and other cores are indicated in triangles.

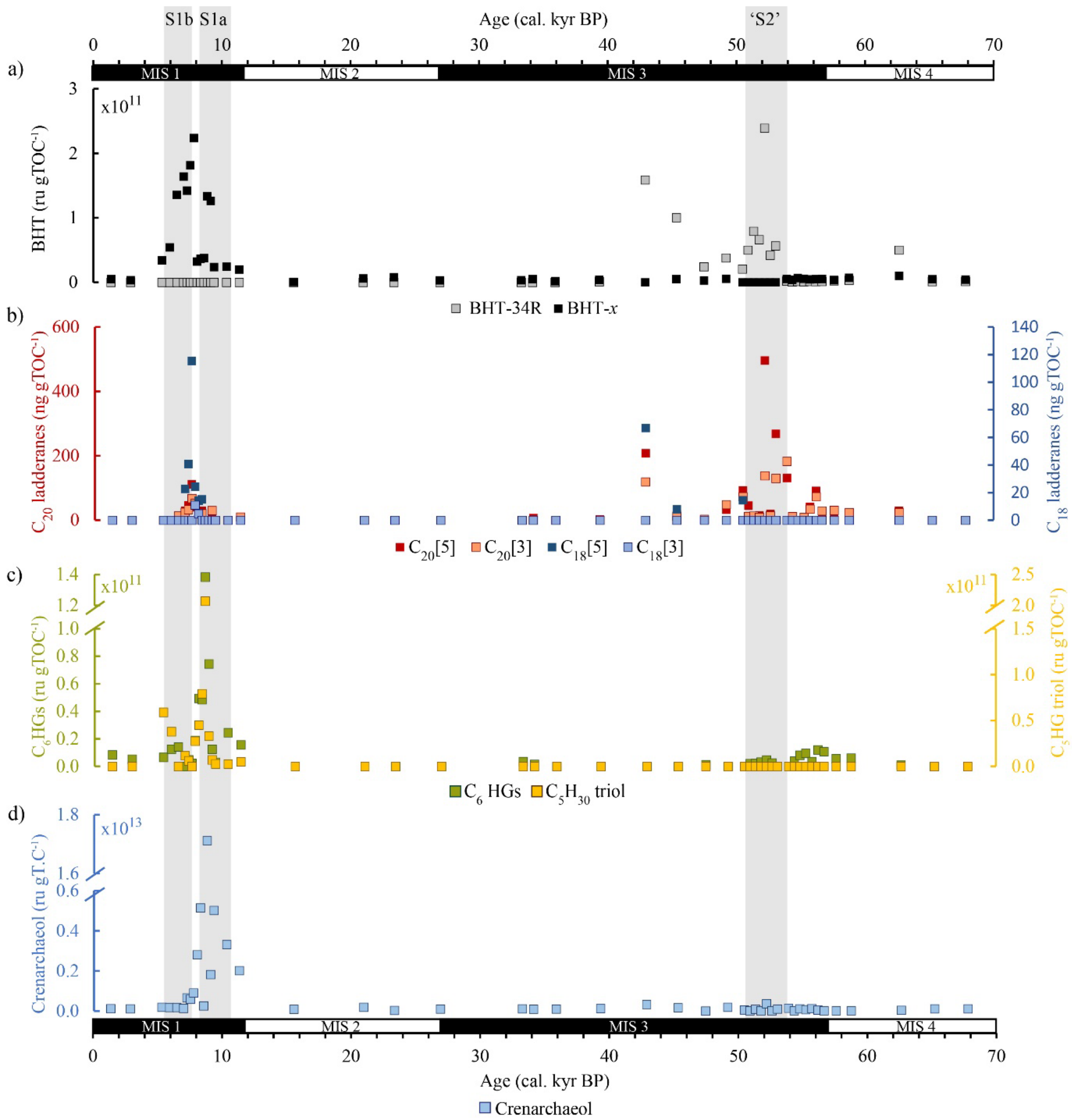

Fig. S2: Lipid biomarker concentrations (normalized against gTOC) at site 64PE406-E1: a) bacteriohopanetetrol (BHT)-x and BHT-34R [rug TOC^{-1}], b) C_{18}[3]-, C_{18}[5]-, C_{20}[3]- and C_{20}[5]-ladderane FAs [ng $gTOC^{-1}$], c) Heterocyte glycolipids (HGs) with summed C_6HGs (C_6HG_{26} diol, C_6HG_{28} diol and C_6HG_{30} triol) plotted on the right y-axis and C_5HG_{30} triol plotted on the left y-axis [ru $gTOC^{-1}$], and d) crenarchaeol [ru $gTOC^{-1}$].

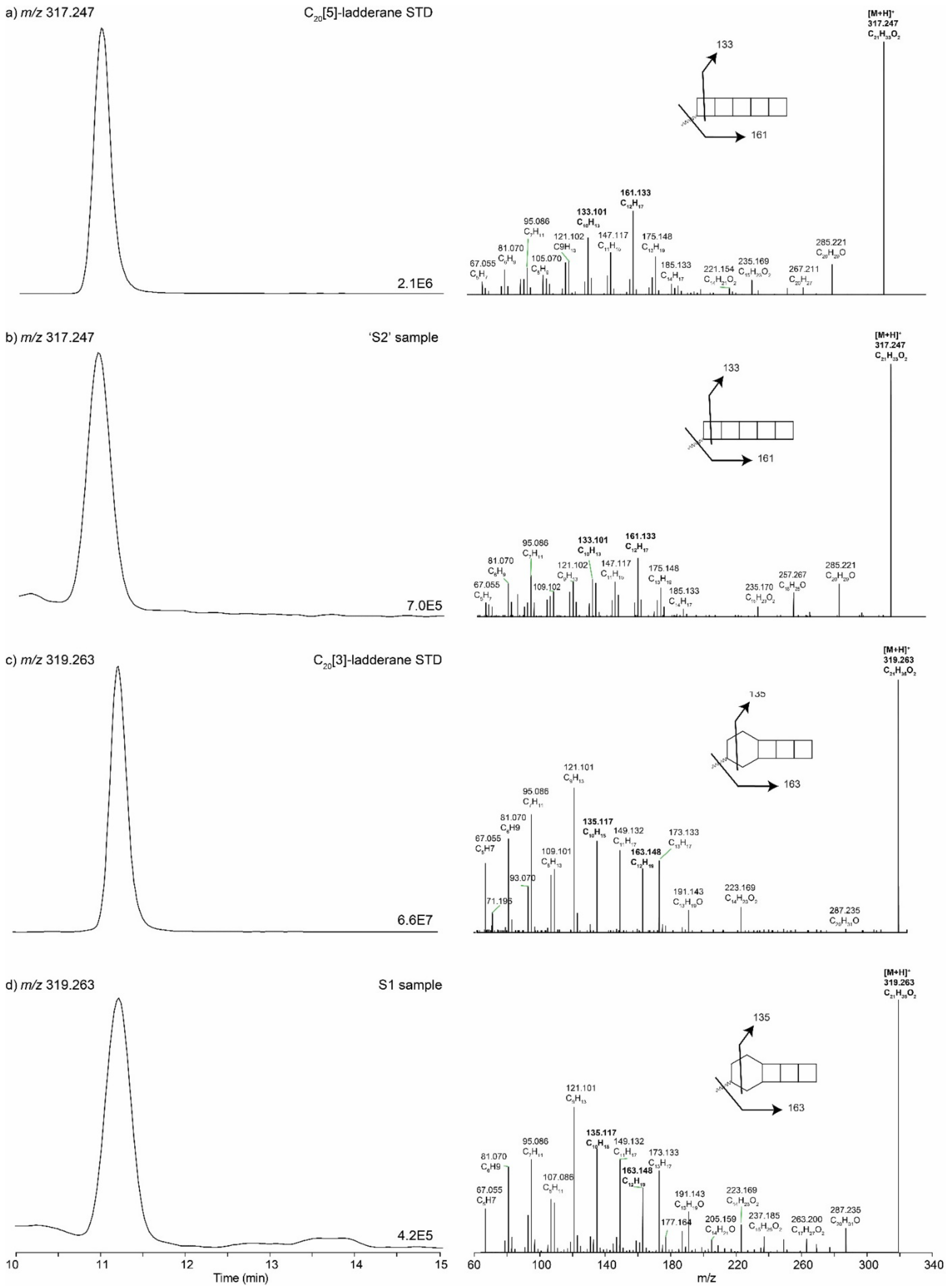

Fig. S3: Mass chromatograms (within 3 ppm mass accuracy) and MS^2 of: (a) C_{20}[5]-ladderane standard, (b) C_{20}[5]-ladderane detected in a sediment horizon recovered from the timing associated with S2, (c) C_{20}[3]-ladderane standard and (d) C_{20}[3]-ladderane detected in a sediment horizon recovered from S1. Characteristic fragments in MS^2 are indicated in bold.

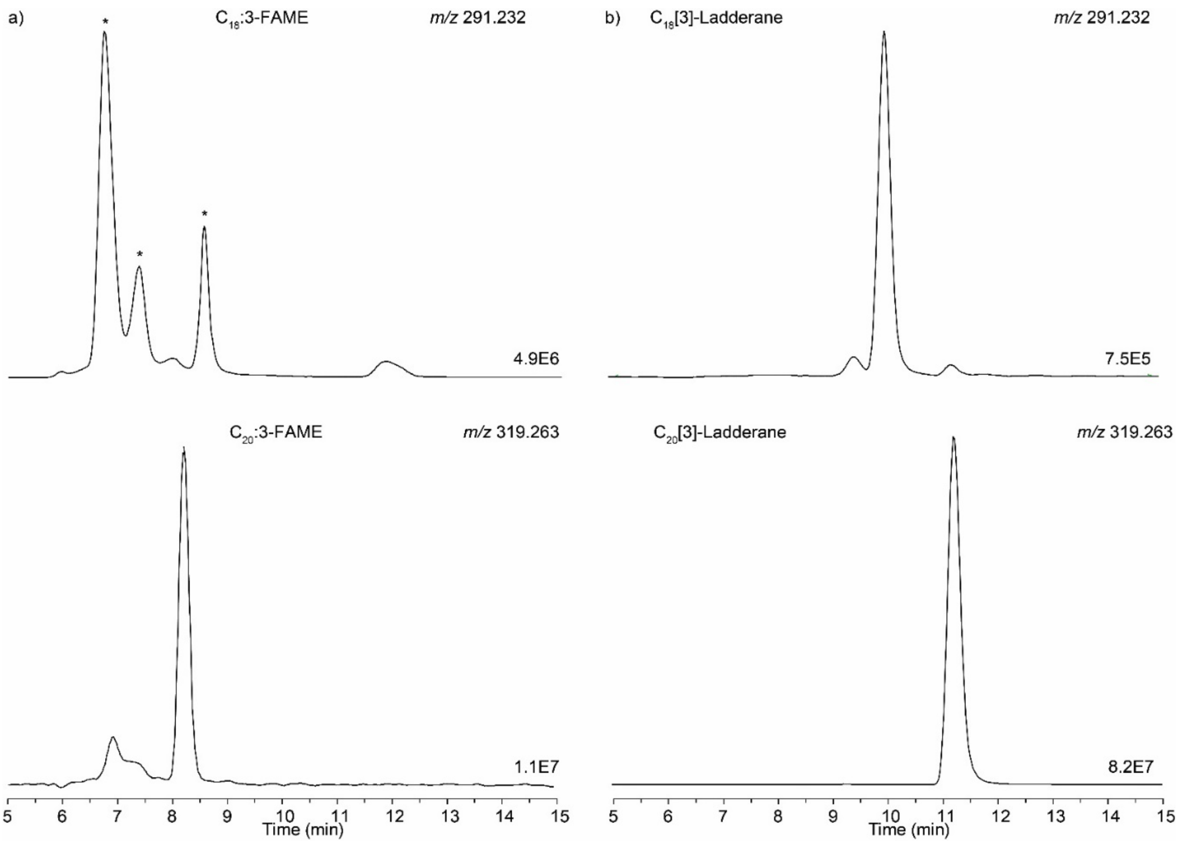

Fig. S4: Mass chromatograms (within 3 ppm mass accuracy) of: a) $C_{18:}$3-fatty acid methyl ester (FAME) in the upper panel and $C_{20:}$3-FAME in the lower panel, and b) C_{18}[3]-ladderane (upper panel) and C_{20}[3]-ladderane (lower panel) in a biomass sample of *Ca.* Kuenenia. Isomers of the same compound are indicated with *. Note that retention time offsets between $C_{18:}$3-FAME/ C_{18}[3]-ladderane and $C_{20:}$3-FAME/ C_{20}[3]-ladderane are 2 to 4 and 3 minutes, respectively.

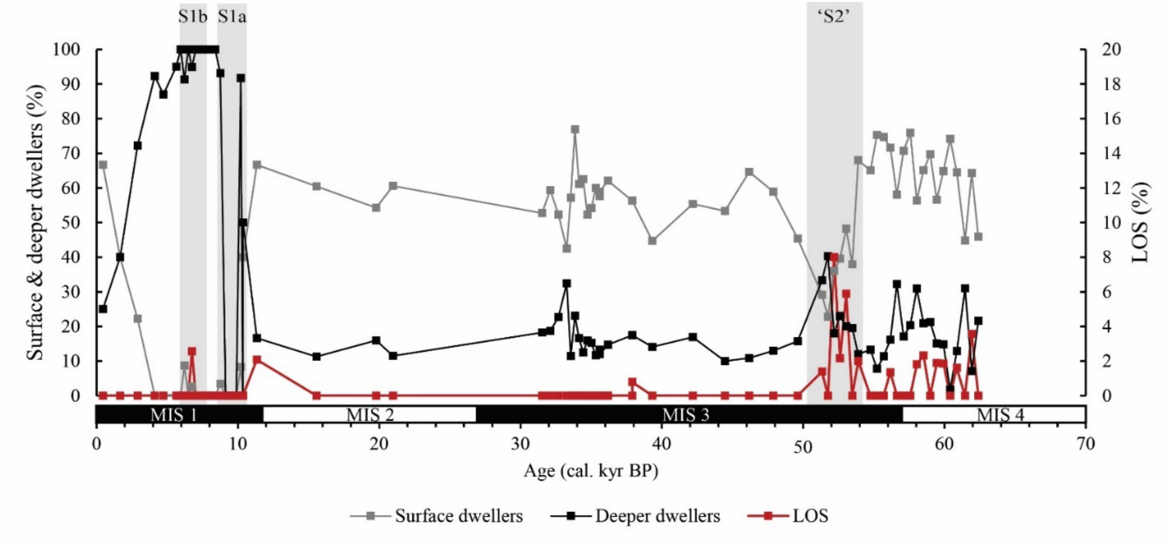

Fig. S5: Relative abundances (%) of benthic foraminifers with species living in surface and sub-surface sediments plotted on the left y-axis and low oxygen indicator species (LOS) plotted on the right y-axis. Timing of S1a, S1b (Rohling et al., 2015; Grant et al., 2016) and the interval associated with S2 (Muerdter et al., 1984), are shown in grey.

References

Clarkson, M. O., Hennekam, R., Sweere, T. C., Andersen, M. B., Reichart, G.-J., and Vance, D. (2021) Carbonate associated uranium isotopes as a novel local redox indicator in oxidatively disturbed reducing sediments. *Geochim. Cosmochim. Acta* **311**, 12–28.

Grant, K., Rohling, E., Bar-Matthews, M., Ayalon, A., Medina-Elizalde, M., Ramsey, C. B., Satow, C., and Roberts, A. (2012) Rapid coupling between ice volume and polar temperature over the past 150,000 years. *Nature* **491**(7426), 744.

Hennekam, R., van der Bolt, B., van Nes, E. H., de Lange, G. J., Scheffer, M., and Reichart, G. J. (2020) Early‐Warning Signals for Marine Anoxic Events. *Geophys. Res. Lett.* **47**(20), e2020GL089183.

Rohling, E. J., Hibbert, F. D., Williams, F. H., Grant, K. M., Marino, G., Foster, G. L., Hennekam, R., De Lange, G. J., Roberts, A. P., and Yu, J. (2017) Differences between the last two glacial maxima and implications for ice-sheet, δ18O, and sea-level reconstructions. *Quat. Sci. Rev.* **176**, 1–28.

Zwiep, K. L., Hennekam, R., Donders, T. H., Van Helmond, N. A., De Lange, G. J., and Sangiorgi, F. (2018) Marine productivity, water column processes and seafloor anoxia in relation to Nile discharge during sapropels S1 and S3. *Quat. Sci. Rev.* **200**, 178–190.